Print ISSN 2710-0200 *Full text available online at* *Ethiop J Nat Comp Sci.*
Electronic ISSN 2710-0219 *http://journal.uog.edu.et/index.php/EJNCS* *Vol. 2 (2) 342-360*
https://doi.org/*10.20372/ejncs/Ge.2022.32*

ORIGINAL RESEARCH

Electrical Resistivity Sounding, Seismic Refraction and Magnetic Surveys for Characterization of a Building Site foundation at Bure campus of Debremarkos University, Ethiopia

Temesgen Ayenew[1*] and Fekadu Tamiru[2]
[1]Department of Geology, CNCS, University of Gondar, Ethiopia.
[2]Department of Geology, CNCS, Wollega University, Nekemte, Ethiopia
*Corresponding author Email: temesgenUoG4310@gmail.com

Received: 23 December 2021/ Accepted/ 29 July 2022; Published online: 15 August 2022
© The Author(s) 2022

Abstract

This study aimed at evaluating the near-surface lithologies at the site selected for building the newly established Bure Campus of the Debre Markose University. To characterize the foundation conditions, integrated geophysical surveys involving Vertical Electrical Sounding (VES), seismic refraction, and magnetic methods were employed. The electrical survey results show the presence of a relatively high resistivity topsoil, a low resistivity clayey soil as a second layer underlain by an intermediate resistivity bed represented by highly to moderately weathered bedrocks with intermediate resistivity, a very conductive highly fractured basalt, and at the bottom highly resistive slightly weathered basalt. The seismic refraction survey mapped top, low -velocity layers corresponding to top dry soil and clayey soil, an intermediate velocity bedrock, and relatively dense, highly fractured basalt. Magnetic anomaly maps and sliced-stack sections delineate the contact between rocks affected by different degrees of weathering while analytical signal and tilt derivative maps have mapped the weak zones resulting from subsurface structures. The correlation of the magnetic anomaly maps, geo-electric sections, and seismic refraction models were used for determining the thickness of clayey soil, the depth to the bedrock, the morphology of competent rocks, areal coverage of relatively highly weathered and fractured rocks and for the identification of weak zones at the site. Finally, the study showed that subsurface materials at the central portions of the study area would have lower bearing capacity for building foundation than the rest of the area based on the anomaly signature mapped by the three geophysical methods.

Keywords: Building site foundation, Vertical Electrical Sounding, seismic refraction, Low Velocity Layer, magnetic anomaly, slice-stacked section

Introduction

With the growing demand for site development and unsuccessful experience of building failure, human beings come up with the art of proper designing and construction of infrastructures to complement their basic needs and future purposes with consideration for the competency of the Earth materials over which the structures will be erected (Ibitoye et al., 2013). All structures constructed on the Earth surface directly or indirectly have their own substructure (foundations) that are supported by soils and rocks (Bell, 2007). The

Print ISSN 2710-0200 Full text available online at *Ethiop J Nat Comp Sci.*
Electronic ISSN 2710-0219 *http://journal.uog.edu.et/index.php/EJNCS* *Vol. 2 (4) 342-360*
https://doi.org/xxxxxxxxxxxxxxxxxxx

ORIGINAL RESEARCH ARTICLE

Electrical Resistivity Sounding, Seismic Refraction and Magnetic Surveys for Characterization of a Building Site foundation at Bure campus of Debremarkos University, Ethiopia

Temesgen Ayenew[1*] and Fekadu Tamiru[2]
[1]Department of Geology, CNCS, University of Gondar, Ethiopia.
[2]Department of Geology, CNCS, Wollega University, Nekemte, Ethiopia

*Temesgen Ayenew, Email: temesgenUoG4310@gmail.com

Received: 08 July 2022; Accepted: 03 December; Published online: 18 Junuary 2023
© The Author(s) 2023

ABSTRACT

This study aimed at evaluating the near-surface lithologies at the site selected for building the newly established Bure Campus of the Debre Markose University. To characterize the foundation conditions, integrated geophysical surveys involving Vertical Electrical Sounding (VES), seismic refraction, and magnetic methods were employed. The electrical survey results show the presence of a relatively high resistivity topsoil, a low resistivity clayey soil as a second layer underlain by an intermediate resistivity bed represented by highly to moderately weathered bedrocks with intermediate resistivity, a very conductive highly fractured basalt, and at the bottom highly resistive slightly weathered basalt. The seismic refraction survey mapped top, low -velocity layers corresponding to top dry soil and clayey soil, an intermediate velocity bedrock, and relatively dense, highly fractured basalt. Magnetic anomaly maps and sliced-stack sections delineate the contact between rocks affected by different degrees of weathering while analytical signal and tilt derivative maps have mapped the weak zones resulting from subsurface structures. The correlation of the magnetic anomaly maps, geo-electric sections, and seismic refraction models were used for determining the thickness of clayey soil, the depth to the bedrock, the morphology of competent rocks, areal coverage of relatively highly weathered and fractured rocks and for the identification of weak zones at the site. Finally, the study showed that subsurface materials at the central portions of the study area would have lower bearing capacity for building foundation than the rest of the area based on the anomaly signature mapped by the three geophysical methods.

Key words: Building site foundation, Vertical Electrical Sounding, seismic refraction, Low Velocity Layer, magnetic anomaly, slice-stacked section

Introduction

With the growing demand for site development and unsuccessful experience of building failure, human beings come up with the art of proper designing and construction of infrastructures to complement their basic needs and future purposes with consideration for the competency of the Earth materials over which the structures will be erected (Ibitoye *et al*., 2013**).** All structures constructed on the Earth surface directly or indirectly have their own substructure (foundations) that are supported by soils and rocks (Bell, 2007). The

sustainability of multipurpose buildings are mainly controlled by the nature of underlying earth materials. For this purpose, site investigation involving exploration of the subsurface conditions, have to be done (Anon, 1999 as cited in Freitas, 2007).

Investigation with limited and sparsely spaced boreholes cannot give deep and sufficient information about the physical property of the heterogeneous subsurface geology. Therefore, geophysical methods are applied to study the physical property of the subsurface to the required depth and provide inputs on suitability of the foundation for the proposed engineering structures. Different ground geophysical methods are used for engineering site investigations, primarily electrical resistivity, seismic refraction, and magnetic methods (Tigistu & Alemayehu, 2014). Among the resistivity survey techniques, the Vertical Electrical Sounding (VES) is the most commonly used survey technique but it does not take into account lateral changes in layer resistivity (Loke, 2001). Considering the complexities of the both laterally and vertically, attempts are made by taking more VES points with known separations to generate geoelectric sections along definite profiles. Geoelectric sections can be used for mapping the electrical resistivity property of the subsurface soils and rocks in two dimensions. Seismic refraction and magnetic methods can be used in mapping subsurface structures, discontinuities and weak zones, and to know the depth of a particular rock or soil during site investigation (Thomas, 2003 as cited Tigistu & Alemayehu, 2014; Emmanuel, 2015).

In areas, where dense multipurpose buildings are proposed, investigations using integrated geophysical methods are very important to know the subsurface condition and propose the appropriate foundation type. The present study area is covered by residual soil but the well log data near to the site and nearby river cut exposures show the presence of black cotton soil at shallow depth which is dangerous to engineering structures. For this reason, this study aims at characterizing the subsurface condition underlying the proposed building foundation in the Bure campus of the Debre Markos University using electrical resistivity, seismic refraction, and magnetic methods.

The study area

The site is located about 400 Km north of Addis Ababa in Western Gojjam Zone, Bure Town between 1184500m-N to1185000m-N, and 289700m-E to 290400m-E (UTM Coordinates).

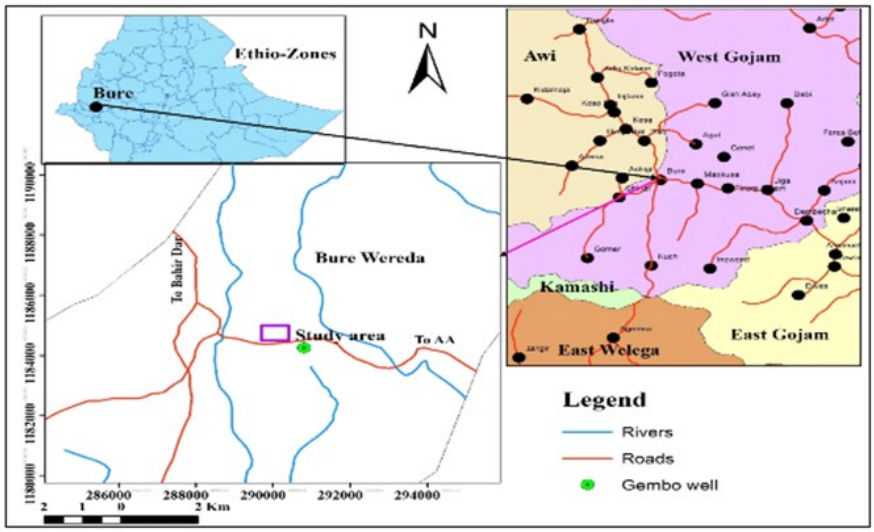

Figure 1. Location map of the study area.

Geology and Tectonics

Cenozoic volcanic rocks

The oldest and most extensive group of volcanic rocks are the, *Trap Series*, erupted from fissures and consisted of piles of flood basalts and minor ignimbrites (Mohr, 1963). The Trap These rocks are overlain by shield volcanoes mainly of porphyritic amygdaloidal olivine basalt (Tadese *et al.*, 2003)**.**

Tertiary and quaternary volcanic spread over the northern and eastern high land plateau and north- central lowland plateaus covering 25% of the whole area of the Bure map sheet and are weathered, fractured, and faulted mainly by trend NE-SW and NS faults (ADSWE, 2017). According to EIGS (2008), the Tertiary volcanic rocks succession in the Bure map sheet comprises lower and upper basalt units, agglomerate, trachyte flows and plugs, thin scoriaceous basalt flows, and scoriaceous basaltic cones.

The most widespread rock unit in the study area is aphanitic basalt, which is exposed along roads, river beds, and quarry sits where there is no overburden or eroded. This unit is weathered and fractured to different degrees. Drilling data obtained from the area close to present study site revealed that the degree of weathering of this unit gradually decreases to depth of 34m while the degree of fracturing increases. Nevertheless, at places, also moderately weathered, but highly fractured rocks are found exposed through which springs are discharging.

Volcano-sedimentary and Quaternary sediments

Sedimentary and volcano-sedimentary rocks are intercalated in various proportions with several volcanic episodes occurring from the early Tertiary to the Quaternary (Tadese *et al*., 2003). Late tertiary to Quaternary sedimentary rocks and sediments associated with volcanic rocks include limestone, siltstone, sandstone, conglomerate, clay, silt, sand, gravel, tuffs, and marls (Tefera *et al.*, 1996 b**)**.

According to EIGS (2008), recent Quaternary superficial deposits occur relatively extensively in the central north and eastern part of the Bure map sheet developed mainly from the underlying Tertiary volcanic rocks. They are grouped into eluvial and alluvial soil covers. The eluvial soil covers most of the plateau area of the Bure area including the present study area. The top part of this soil is generally, red to reddish-brown silty to sandy soil commonly containing basalt rock fragments. The red and reddish-brown color of the residual soil may indicate its in situ development from the underlying basaltic rocks.

The alluvial soil occurs along the flanks of Yisir River, in marshy areas, and in areas where the top residual soil is eroded away, particularly to the south of the present study area. It is commonly black cotton soil and rarely dark brown silty soil. During the summer season, the pore spaces in this soil are oversaturated with water but during the dry season, large cracks are observed on this soil. As a result, this soil is characterized by its swelling (during summer season) and shrinking (during dry season) properties and is very dangerous for buildings.

According to EIGS (2008), the regional structural setup of the Bure area includes a relic of early folds and foliations or migmatitic layering, N-trending regional foliation, folding of this N-trending regional foliation and associated lineation, and the brittle-ductile shear zones, N-S and NE-SW (graben forming) trending normal faults. Lineaments traced from aerial photographs and satellite imagers generally show NW-SE, NE-SW, N-S, and E-W trends and are found in all rocks.

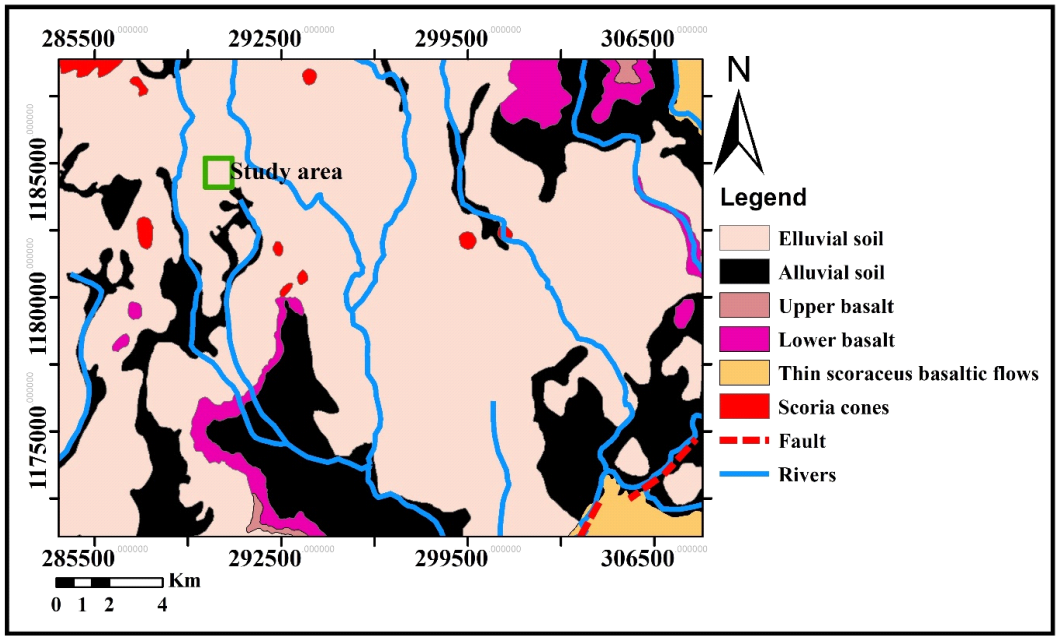

Figure 2. Geology of the study area and its surrounding (modified from EIGS, 2008)

Materials and Methods

Data acquisition and instrumentation

Electrical Resistivity Sounding

The Vertical Electrical Sounding (VES) technique was carried out with the Schlumberger array employing the ABEM Terrameter LS instrument. This technique is based on injection of electrical current (I) into the ground through two current electrodes and measuring the resulting potential difference (V) by another pair of potential electrodes placed close to the center of the array. The instrument then directly displays the corresponding apparent resistivity at that station.

A total of sixteen sounding stations were occupied along four profiles oriented in E-W direction (Figure 4). The Garmin GPS 72 was used to locate the position of these sounding points. The maximum current electrode spacing of AB/2 133m was used and repeated measurements were taken at AB/2 equals 10, 13.3, 75, and 100m to examine the data quality and assess the effect of any possible anisotropic character of the underlying formations. Hence the method measures only the vertical variation of resistivity of subsurface materials four VES points were collected in each profile to construct pseudo-sections and geo-electric sections for later interpretation.

Magnetic survey

A proton precession-600 magnetometer was used to measure the total magnetic field at different points in the area. A total of 194 magnetic data were collected in three days with a station interval of 20 and 30 meters in 8 profiles oriented in E-W and NW-SE directions to cover the area. At each station, the magnetometer reading, recording time, location in UTM coordinates, and elevation in meter were recorded. Every reading was taken away from magnetic materials such as cars, fences, houses, power lines, and walls made of basic rocks. A base station reading was taken every day to take diurnal correction.

Seismic Refraction Survey

The objective of the refraction seismic survey was to determine the velocity of elastic

waves propagating along different paths within the subsurface and indirectly to assess the density characteristics. Every wave reaching the geophone produces a momentary impulse on a record of ground vibration called a seismogram.

The survey was conducted in 4 profiles using a 24 channel ABEM TERALOCK MK 6 seismic recording system. The geophones were connected to the seismograph via seismic cables. The data were collected in four profiles each containing three spread lines to cover the available area (Figure 4). Spread 3 and 9 have a geophone spacing of 3m, spreads 4-6 have a geophone spacing of 4m and the other spreads have a geophone spacing of 5 m. Accordingly, the spreads have a length of 69, 92, and 115m respectively. A 10kg sledgehammer was used as a source to generate elastic waves. The sledgehammer was connected to the seismograph using the trigger cable to arm the seismograph as the impact is done. The field procedure employed was an in-line spread in which the source and the geophones were placed in a straight line. Five to seven shot points were selected for a spread resulting in 15-21 shot points on a profile. The location of the shots was 0m, 17.5m, 34.5m 52.5m, and 69m for spread, 3, and 9, 0m, 23m, 46m, 70m, and 92m for spreads 4, 5 and 6, and 0m, 27.5m, 57.5m, 87.5m, and 115m for other spreads. At each shot point location, coordinates and elevation data were recorded using Garmin GPS 72.

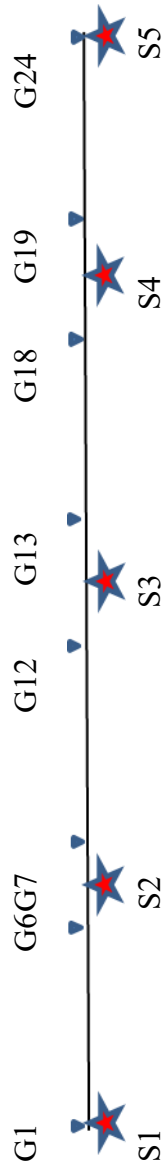

Figure 3. A general arrangement of seismic wave receivers (G1-G24) and sources (S1-S5) employed for the present study

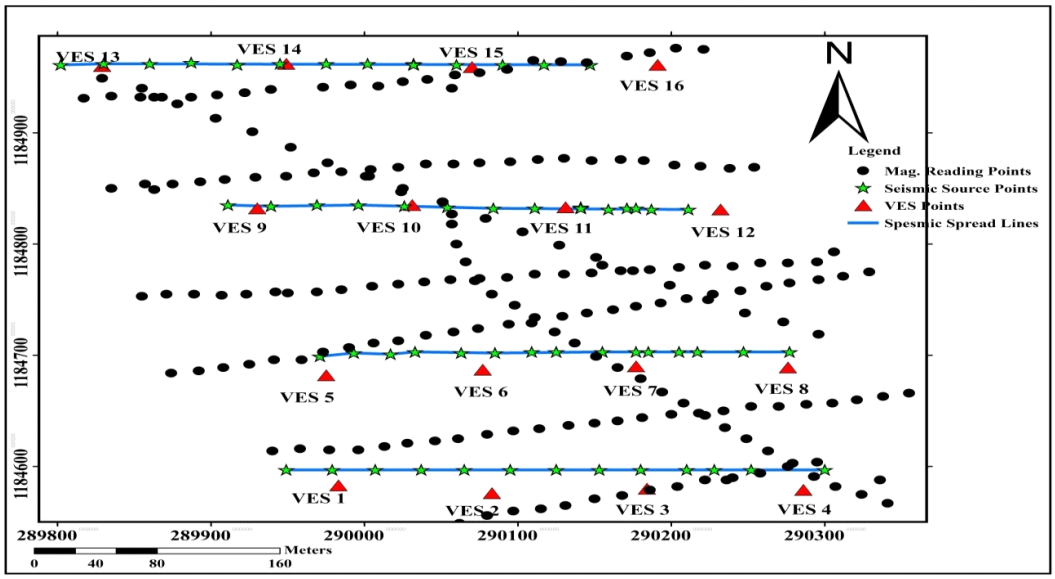

Fig.4. Geophysical survey layout

Data processing

The data collected were processed and analyzed using IPI2Win, IPI_re3, and surfer 10 software programs, and presented as curves, pseudo-sections, geo-electric sections, and sliced stacked maps. Two basic parameters were determined; resistivity and thickness of layers. For AB/2 of 133 meter, the processed curves show five subsurface layers. These curves were used as input data for IPI_re3 and surfer 10 to construct geo-electric sections by connecting VES point resistivity values taken from one profile. In addition, pseudo-depth sections and sliced staked maps of apparent resistivity data were produced using surfer 10 to see the general variation of apparent resistivity in a profile and in the whole survey area respectively.

The magnetic data processing started by correcting the raw data for diurnal variation. The observed magnetic data were corrected for diurnal variation according to equation (1). Diurnally corrected magnetic data were processed using Oasis Montaj V6.4.2 software. A total magnetic field anomaly map was then produced to see the magnetic field variation in the survey area. For better interpretation of magnetic data enhancement techniques, analytical signal and tilt derivative methods were applied.

$$T_c = T_i \pm \frac{(T_2 - T_1)}{(t_2 - t_1)}(t_1 - t_1).....(1)$$

Where T_1 and T_2 are magnetic field readings at the base station at the beginning and at the end of the magnetic survey, t_1 and t_2 are the corresponding time respectively. T_c is the corrected magnetic data, T_i is magnetic data observed along the traverse, t_i is the corresponding time.

PickWin95 and Plotrefa software programs were used to process seismic refraction data. Raw field data in 'seg2' format were imported into PickWin95 and the first arrivals of the P-waves were chosen. A band pass filter frequency of 56.9Hz low cutoff and 409.6 Hz high cutoff were applied to take out the low and high-frequency noise. These cutoff frequencies were chosen considering the range of seismic frequencies and observing the seismogram (waveform). This was performed for each of the shot points along the spreads. The first arrival picked data were imported into Plotrefa, and a plot of time versus distance was generated. Plotrefa automatically checks reciprocal times for

multiple shot locations. Most of the data points presented in this work show RMS errors below 5%.

Layers were assigned by identifying crossover points, which occur where the slope (1/v) changes. After the layer assignment, a time-term inversion was done. An initial velocity model generated from quick time term inversion was used as an input parameter for the tomographic inversion and for generating a layered model. Velocity sections of the subsurface and corresponding depth were generated along respective profile.

Results and Discussion

Geo-electric sections

All geo-electric profiles run almost parallel to each other and are oriented in the east-west direction. The first three profiles cover 300 m survey length each while the fourth profile has a length of 360 m. Profile-1 is found in the southern whereas Profile-4 in the northern part of the area. The geo-electric layers were described in terms of layer resistivity, thickness, and depth. Each layer is named based on the nearby borehole data. The upper most layer (with a resistivity of 69.8 to 220.2 Ωm and a thickness of 0.7 to 1.3 m) is more likely to be a mixture of top dry soils. It is relatively thick along Profile-1 compared to other profiles. The lateral variation in the resistivity and thickness of this layer is believed to be due to the variation in the compactness of the soil. The low resistivity (32 to 63 Ωm) corresponds to clayey soil with a thickness range of 0.7 to 5.4m. The maximum thickness is observed beneath VES 12**.** The intermediate layer is characterized by slightly higher resistivity range (66-120 Ωm)**.** This layer has a nearly similar electrical response to the first layer and resembles highly to moderately weathered and fractured basalt. It has characterized by irregular morphology with minimum thickness and depth to the layer detected beneath VES 15 (is 2.8 m) while the maximum thickness is observed beneath VES 16 (is 17.7 m). The variation in resistivity and thickness of this layer could be due to the variation in the degree of fracturing and/or saturation of the rock in this area (more probably associated with structures).

The fourth layer has very low resistivity (22.3 to 35 Ωm) and can be called moderately weathered and highly fractured scoriaceous basalt as inferred from the borehole data, which is found at about 80 m from the site. As we go to the center of the area the resistivity of this layer decreases, more likely to be due to the high degree of fracturing and fluid saturation with only a small contribution of weathering. The basis of this layer is highly resistive and corresponds to slightly weathered and fractured basalt. However, this layer shows a relatively low resistivity response in profile-3 when compared to the resistivity of the bottom layer in profile-1 and -2. This variation could be due to the variation in the degree of fracturing and fluid saturation. The significance of these two geo-electric layers is to support the bedrock in carrying heavy engineering structures.

Generally, the first two layers (top dry soil and clayey soil) show a relatively high resistivity response along profile -4 when compared to their resistivity in other profiles indicating a relatively lower degree of saturation and clay content. In all profiles, the third layer has an intermediate resistivity response analogous to highly to moderately weathered and fractured basalt and can be considered as the bedrock for a foundation. From an engineering point of view, rocks at the central part of the area have low bearing capacity relative to the rest of the area.

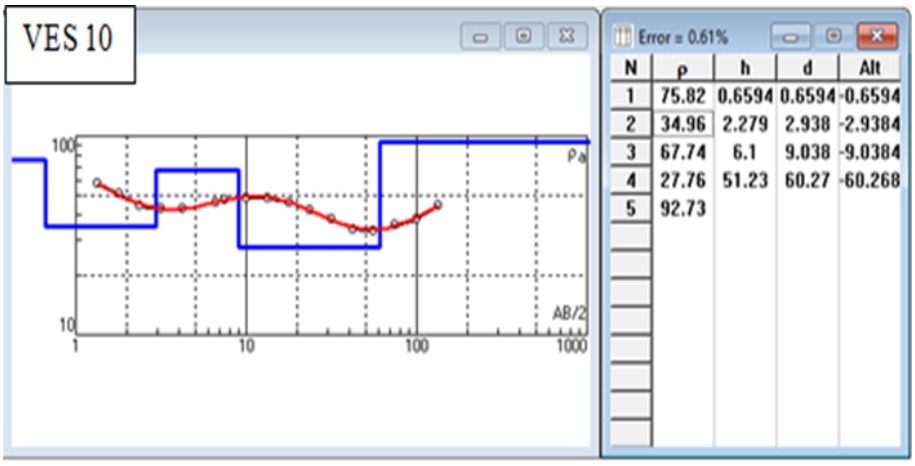

Figure. 5 Typical 1D interpretation of VES.

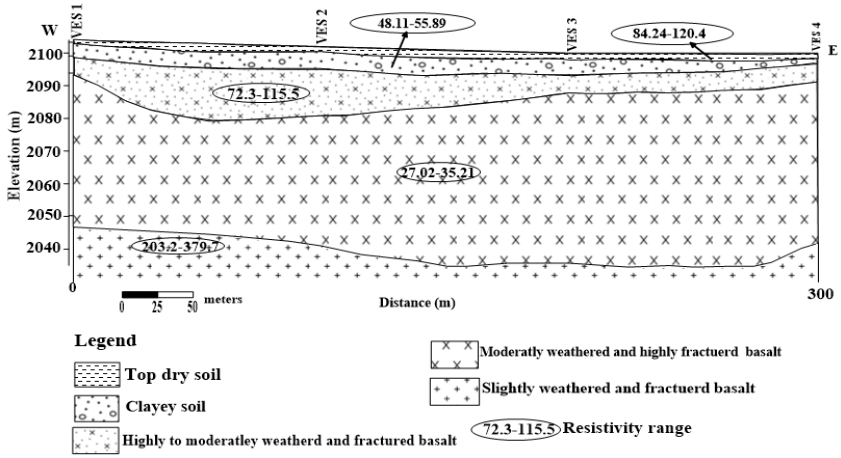

A

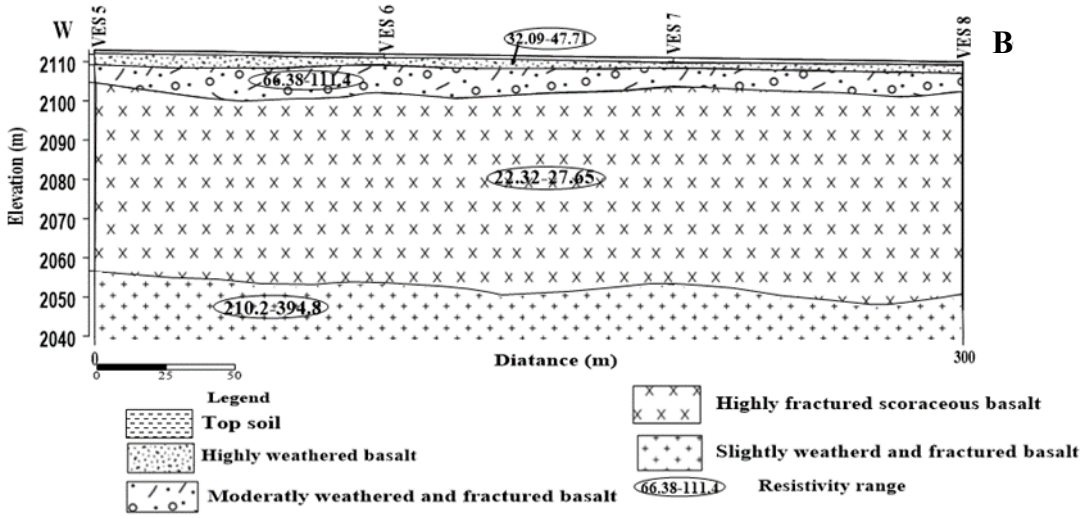

B

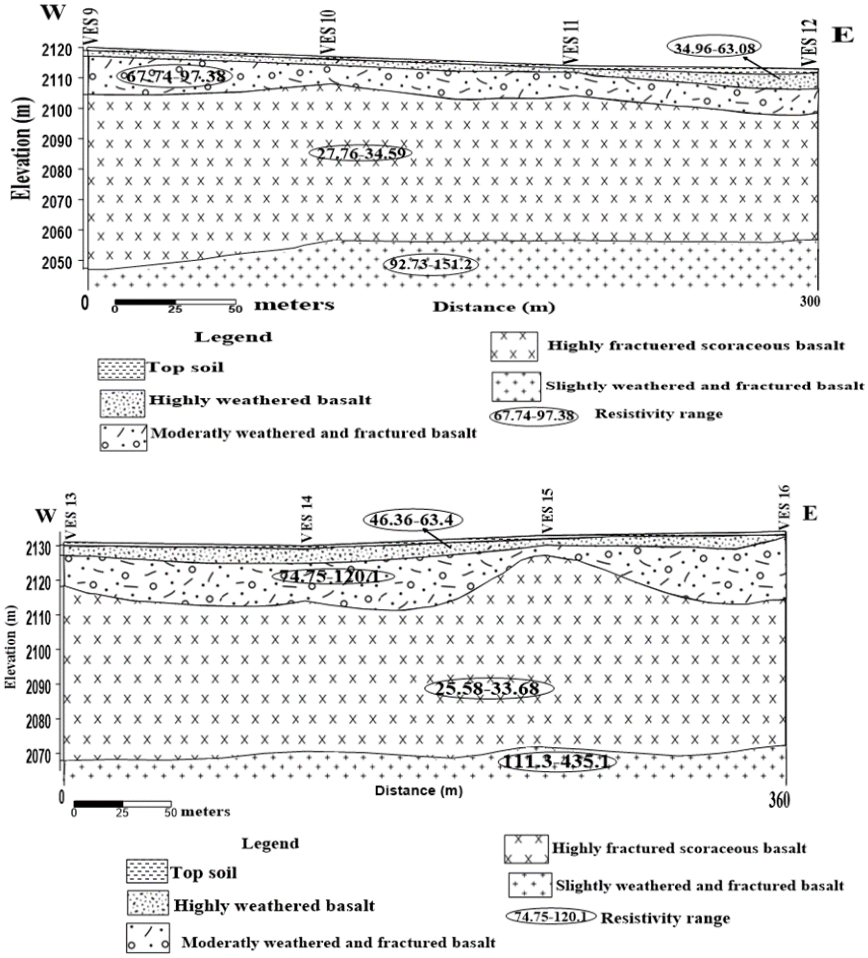

Figure 6. Geo-electric section along (A) profile -1, (B) profile -2, (C) profile -3 (D) profile -4.

Stacked apparent resistivity pseudo-section map

Sliced-tacked apparent resistivity pseudo-section maps were used to see the three-dimensional variation of resistivity in the entire study area and to understand the general subsurface geological outline. These maps were constructed from VES data using resistivity values recorded at different current electrode half spacing. Five sliced maps (at AB/2 of 1.78, 6.62, 17.8, 56.2, and 133m) were prepared and stacked together to obtain a simple image of the subsurface of the present study area based on resistivity variation. These spacings are selected based on the change in resistivity reading at such spacing.

From the sliced-depth and stacked maps shown in Figure 6, it is possible to divide the subsurface setup of the whole area into three regions. A high resistivity zone (Zone 1) covers much of the eastern part of the first sliced map. It is not observed in maps constructed from AB/2 spacing of greater than 1.78m and therefore it is most likely the response of top relatively dry/compacted soil.

Zone 2 is characterized by relatively intermediate apparent resistivity value. This zone is observed in all maps but disappears in a sliced map constructed using AB/2 of 56.2 m.

At the top, its coverage starts from the central part and increases towards the Southwestern region. This is most probably due to the presence of relatively less compacted wet topsoil in these areas. A map constructed at AB/2 of 6.62 m is dominantly covered by the lowest resistivity values of this zone indicating the presence of relatively wet highly weathered material or clay. At AB/2 of 17.8, the higher resistivity values of this zone cover much of the western and northeastern parts of the area. This more likely demonstrates the presence of less weathered material in this zone. Beyond this depth, this zone disappears and reappears again at AB/2 of 133m covering the southern, northern, and Eastern parts of the subsurface area.

Zone 3 is characterized by its low resistivity value and is detected after AB/2 of 6.62. Its area of coverage increases with depth and covers the whole survey area at the third sliced map with very low resistivity value at the central and southeast part of the area. This zone more depicts the presence of highly fractured material. After this depth, the area of coverage of this zone again decreases and the resistivity value increases illustrating a decrease in the degree of weathering and fracturing of subsurface rocks.

In summary, from the stacked resistivity pseudo-depth section maps, less competent bedrock is detected at the central and southeastern part of the study area as highly fractured rocks support it. As result, this part of the study area is less suitable for sitting large size buildings as it may suffer from settlement. In addition, attempting to place buildings in this area need much time and cost for soil treatment. On the other hand, relatively dry and hard bedrock is found in the northeastern part of the area. For this reason, this area is more suitable for the foundation from a resistivity survey point of view.

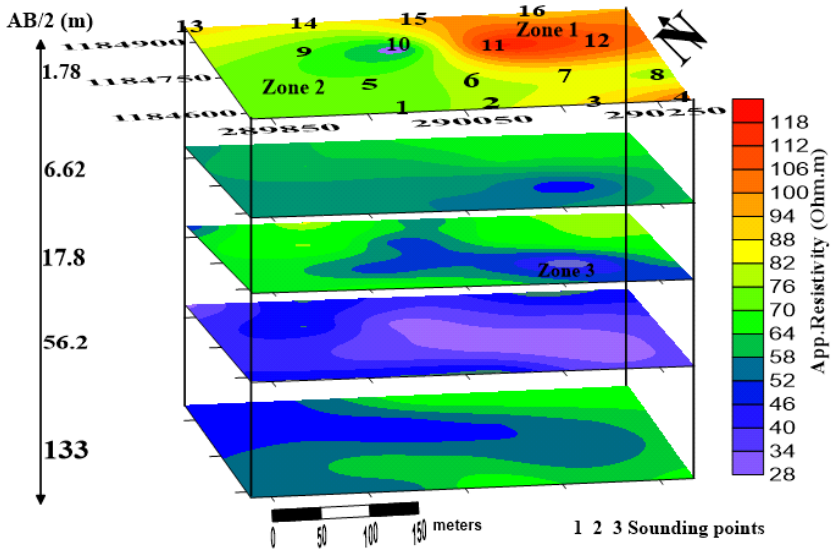

Figure 7. Sliced-Stacked Apparent resistivity pseudo-section map of the entire study area

Interpretation of seismic refraction data

The shallow seismic refraction method gives information about the subsurface in terms of seismic velocities. These velocities depend on the composition, quality, hardness, compaction, and water/gas content of the medium (Telford *et al*., 1990; Kearey *et al.*, 2002). In this work, the calculated seismic velocities are classified into three and are used to identify the subsurface rock layers in the survey

area. In all models, the top layer has low P-wave velocity and can be considered as a low-velocity layer (LVL). According to Sheriff and Geldart (1995), a layer can be called LVL if its P-wave velocity falls in the range of 250 to 1000 m/s and its thickness may extend to 50 m. The base of LVL coincides roughly with the water table, indicating that the low- velocity layer corresponds to the aerated zone (pores filled with gas) above the water-saturated zone.

Seismic Profile-1

From west to east, profile -1 contains spreads 1-3 and covers a total length of 300 m. It is found in the southern end of the survey area along with VES profile-1 (Figure 4). Spread 1 and 2 were taken with geophone spacing of 5 meters but spread 3 was taken with geophone spacing of 3 m. Accordingly, the layered velocity model indicates that the subsurface consists of three major seismic layers up to a depth of 20 m (Figure 7). The first layer has a seismic velocity ranging from 314 to 354 m/s and from the borehole data and resistivity survey result; it could be a combined response of top unconsolidated dry soil and clayey soil. Relatively a uniformly thick deposit of this overburden material is observed in spread 1 and 2 but in spread 3 its thickness increase towards the west. The second layer has a velocity that ranges from 934 to 1347 m/s and extends to a depth of 15 m. This velocity range also includes the third layer of spread 3 and more likely results from highly weathered to moderately weathered and fractured basalt. As a result, the second layer of spread 3 can be considered as highly weathered basalt but the third layer is moderately weathered and fractured basalt. With this consideration, a layer with a velocity of 111 to 1347 m/s can be considered as the best bedrock for the foundation in this profile. However, attempting to put large structures in spread 3 using a shallow foundation will cause differential settlement with the settlement being larger over the greatest thickness of the unconsolidated overburden and highly weathered material (Frietas, 2007). The bottom high - velocity layer (2141 to 2542 m/s) mapped in spread 1 and 2 corresponds to moderately weathered and highly fractured basalt. It is found at relatively shallow depth (10 to 15 m) and can be used to support the overlying bedrock when a heavy structure is erected.

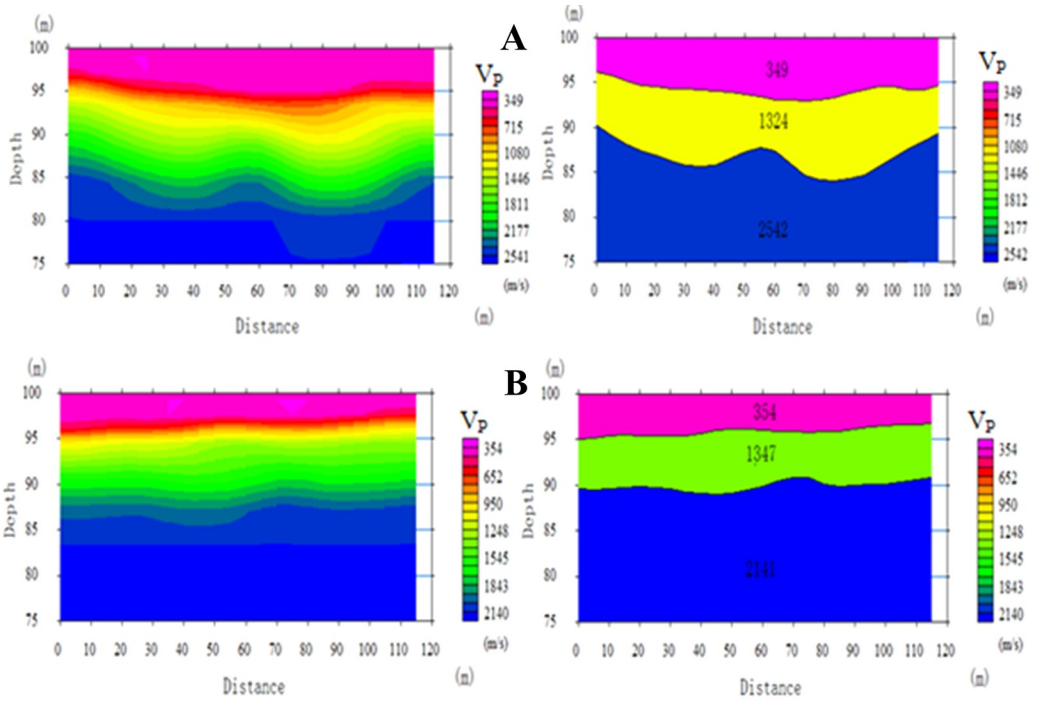

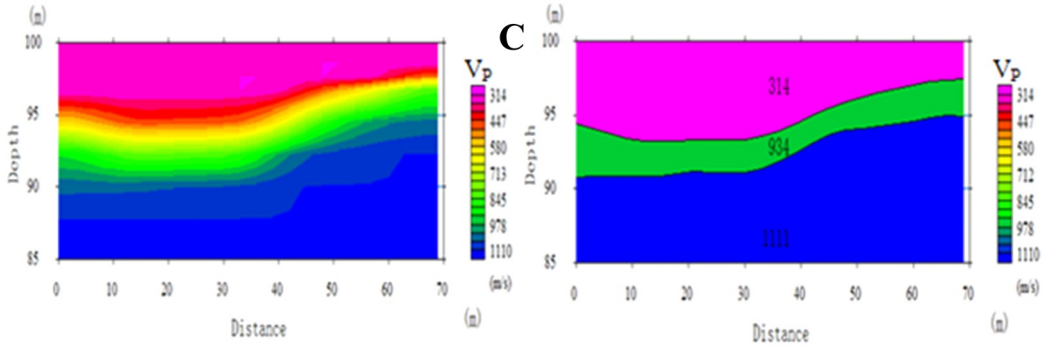

Figure 8. Inverted initial velocity models (left) and layered velocity models (right) obtained from spread 1 (A), spread 2 (B) and spread 3 (C).

Seismic Profile-2

Profile - 2 which is found along with VES profile – 2 (Figure 3) contains spreads 4, 5 and 6 from West to East with a total length of 276 m and geophone spacing of 4 m in each spread. The top layer with a P-wave velocity 271 to 335 m/s extends to a depth of 5 m and represents a combination of unconsolidated dry soil, clayey soil, and/or highly weathered basalt. The thickness of this layer generally increases towards the western end of the profile but its density decreases away from the center. A layer with a P-wave velocity of 1358 to 1397 m/s corresponds to moderately weathered and fractured basalt and can be recommended as the bedrock for a foundation. The unit extends to a depth of 10 m but does not show a large thickness variation along the profile. The third layer

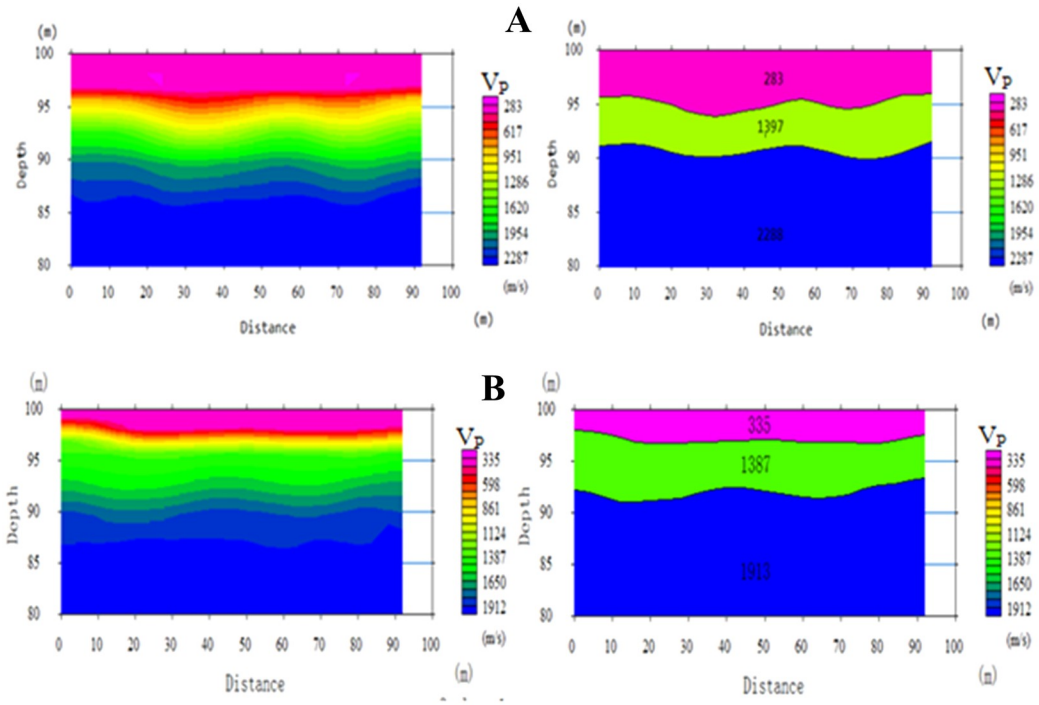

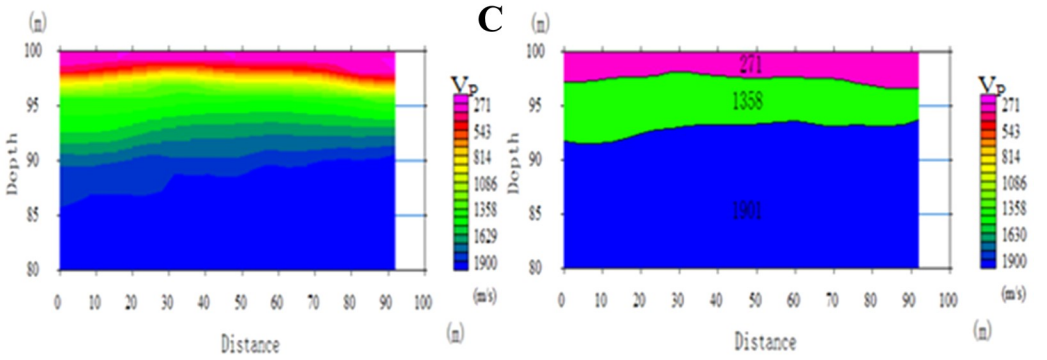

Figure 9. Inverted initial velocity models (left) and layered velocity models (right) obtained from spread 4 (A), spread 5 (B) and spread 6 (C).

Seismic Profile-3

Profile -3 which is found near to VES profile -3 (Figure 3) contains spread 7, 8, and 9 from west to east and covers a total length of 295 m. Spreads 7 and 8 were taken using geophone spacing of 5 m but spread 9 was taken at geophone spacing of 3 m. The velocity model constructed from this profile also show three layers. The top layer has a P-wave velocity of 251 to 308 m/s and extends to a depth of 4 m with slight lateral variation in thickness. This layer resembles unconsolidated dry soil and clayey soil. Below this layer, the velocity of P -waves show a relatively large lateral variation. Similar to the velocity of P-waves in the second layer of profile-1; the P-wave velocity of this layer decreases towards the east. In spread -9 a thin, low-velocity layer is mapped next to the topsoil layer. This is more probably the result of decomposed rock. On the other hand, the third layer of this spread more likely represents a highly weathered basaltic rock and extends to a depth of 12 m. However, the second layer in spread 7 and 8 has a velocity of 1043 m/s and 1161 m/s respectively, and represents an average response of highly to moderately weathered basalt.

In general, the seismic layers mapped in spread 9 are low-velocity layers (LVL). In spread 7 and 8, the second layer can be used as bedrock but for better confidence, it is better to use the third layer as bedrock. However, to identify the best bedrock in spread 9 it is necessary to investigate the subsurface using geophone spacing of greater than 3 m. As a result, proposing to put large structures on the entire area of this profile using shallow, isolated footing will cause differential settlement with the settlement

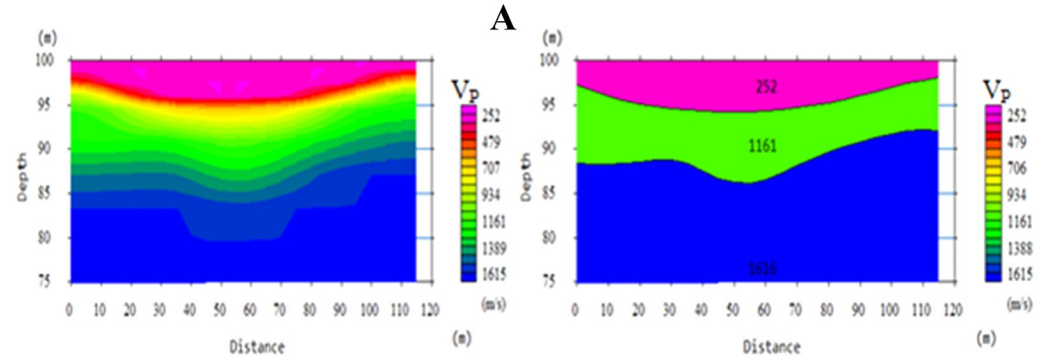

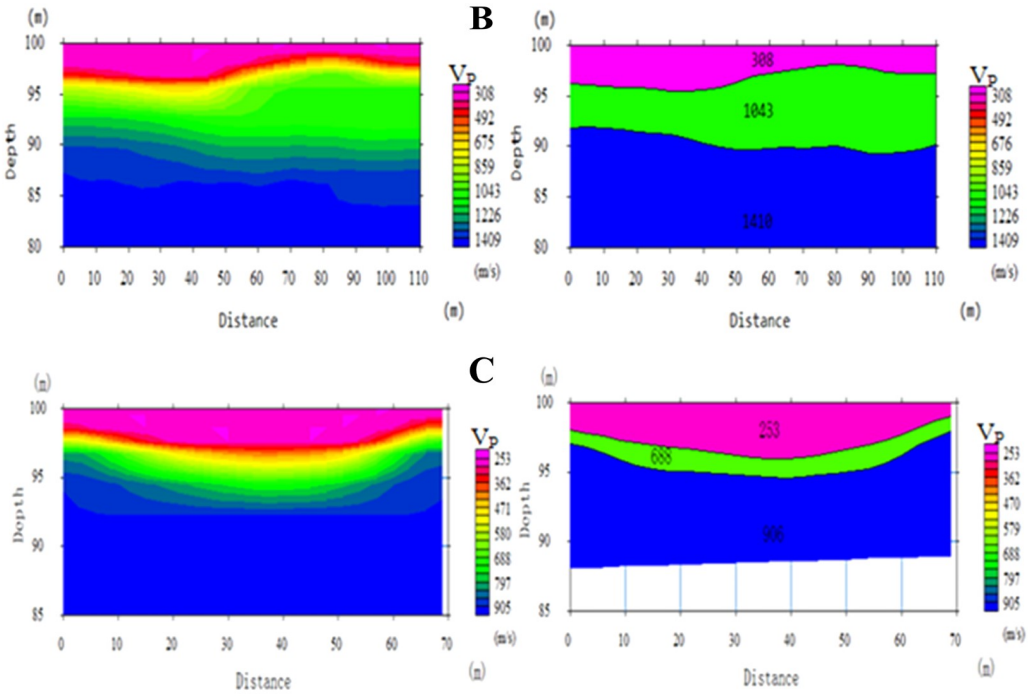

Figure 10. Inverted initial velocity models (left) and layered velocity models (right) obtained from spread 7 (A), spread 8 (B) and spread 9 (C).

Seismic Profile-4

This profile is found in the Northern end of the study area along with VES profile-4 and covers a total length of 345 m. It contains spreads 10, 11, and 12 from West to East. The inverted initial velocity model and layered model show three subsurface layers. The P-wave velocity model in this profile shows a general increase in the velocity of layers towards the east. The low-velocity layer is the response of top unconsolidated dry soil and clayey soil. The thickness of this layer varies laterally but it is generally thick in the eastern part of the profile. The second layer has a P-wave velocity of 1289 to 1325 m/s. This velocity range is the response of highly to moderately weathered and fractured basalt and can be considered as the bedrock in this profile. This layer is characterized by relatively complex morphology and does not have uniform thickness throughout the profile rather its thickness increases towards the ends of the profile. However the rock in spread 11 and 12 are more competent to carry heavy structures.

The third layer shows a relatively high p-wave velocity, 1787 to 2065 m/s. This value represents moderately weathered and highly fractured basalt but the degree of weathering is now smaller than the degree of fracturing in the second layer and the interconnected pore spaces are saturated with water.

In general, from the point of view of the seismic refraction survey result, rocks that have P-wave velocity of less than 1000 m/s will have low bearing capacity. To propose the appropriate foundation type for a building, it is essential to know the depth and thickness of this layer as well as the morphology of the appropriate bedrock. With this respect, rocks in the central part of the study area (seismic profile - 3) shows low bearing capacity and seismic layers in profile -2 have uniform thickness throughout the profile and will not cause differential settlement.

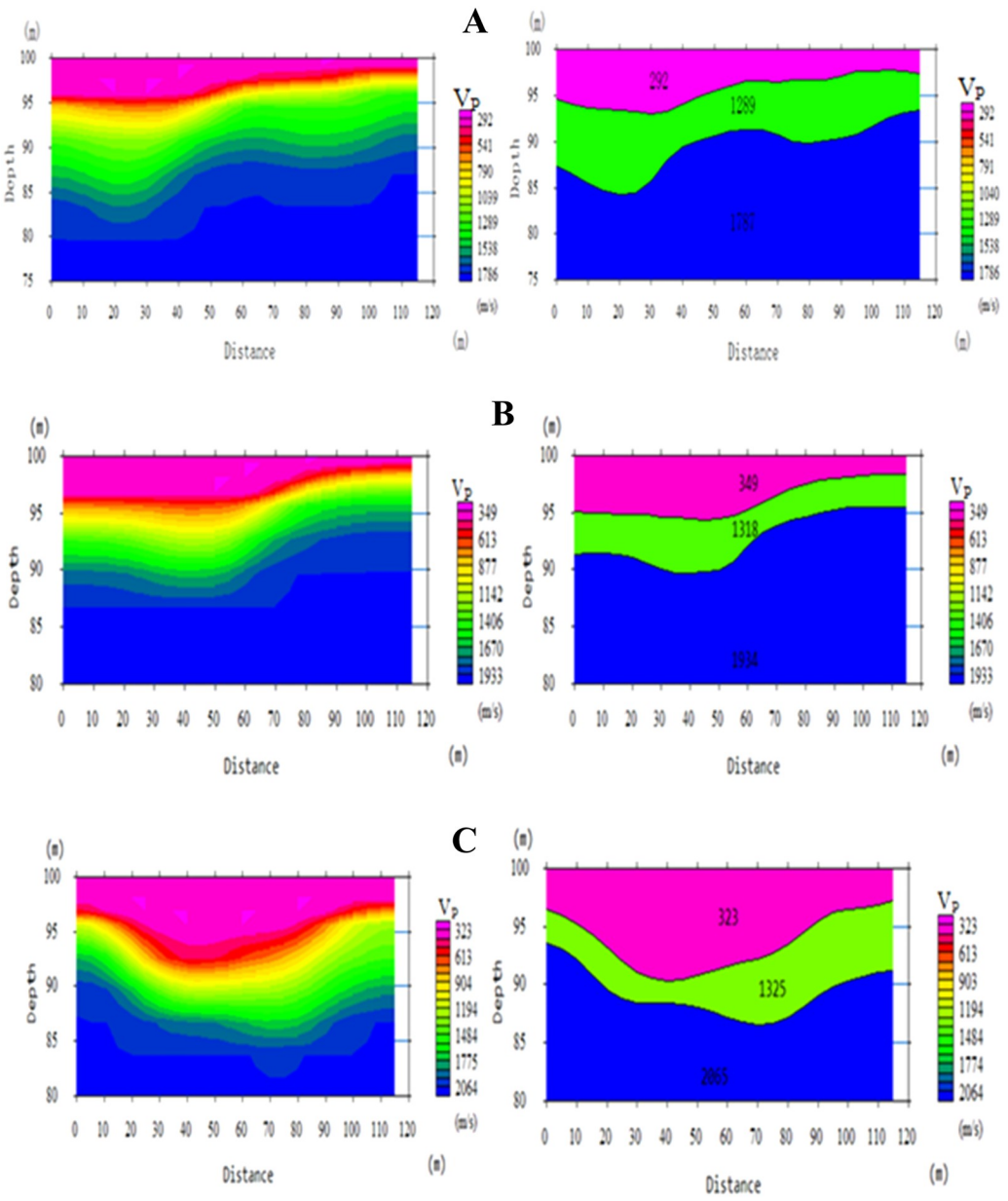

Figure 11. Inverted initial velocity models (left) and layered velocity models (right) obtained from spread 10 (A), spread 11 (B) and spread 12 (C).

Interpretation of magnetic data

After correction for the diurnal variation, magnetic data can be interpreted both qualitatively and quantitatively. The qualitative process is largely map and profile-based and illustrates the general magnetic characteristic of the surveyed area. It involves recognition of discrete anomalous bodies including subsurface structures, discontinuities, weak zones and intrusions using different maps and associated

enhancement techniques. For this work total magnetic anomaly, analytical signal and tilt derivative were used to see the magnetic property of the subsurface materials of the entire study area.

Total magnetic anomaly map

As shown in Figure 8 below the magnetic anomaly map of the study area can be categorized into two zones based on the range of values they show in the anomaly signature. Zone 1 covers most of the Southern and small portion of the Northern part of the study area and is characterized by relatively very high magnetic anomaly response resulting from the presence of highly magnetized bodies that result from the relatively fresh basalt found at a relatively shallower depth. The lowest values of this zone is observed in the central South and Southeastern regions and this could be due to the presence of thick soil deposit and/or weak zones filled with weathered material.

The central part of the study area is characterized by low anomaly response and is represented as Zone 2. These low values of magnetic anomaly in this zone more likely results from high degree of weathering of the underlying rock materials and/or weak zones filled with weathering products (Almadani *et al*., 2014; Olusola *et al*., 2015). As a result it is possible to consider the contact between Zone 1 and Zone 2 as the contact between differently weathered rock materials.

Analytical signal map

The analytic signal map was developed from the total magnetic anomaly map. The technique uses the derivative of magnetic anomalies to determine causative source parameters such as boundaries and plane locations. It is used to improve the clarity of near surface anomalies at the expense of deeper anomalies and is good for locating the edges of shallow bodies. For this reason, the amplitude of simple analytical signal attains maxima over magnetic contacts regardless of direction of magnetization. As a result relatively large NW-SE and small NE-SW oriented weak zones are clearly observed on the analytical signal map shown in the Figure 12B.

In general, the central part of the analytical signal map shows the presence of continuous weak zones at shallow depth. Therefore from the point of view of the magnetic surveys, the areas that show continuous peak analytical values exhibit low bearing capacity due to weak zones/highly fractured, near surface rocks filled with weathered materials.

Magnetic tilt derivative map

The tilt angle derivative is a method developed for balancing or equalizing different amplitude edges. It is the arctangent of the ratio of the vertical derivative of the potential field to its total horizontal derivative. Its amplitude has three rates; positive over the source, zero at or near the edges of the source and negative outside the source. This method produces relatively sharp anomalies and generates better definition of edges over the body. As a result it can be used in mapping geological contacts, faults, dykes and ore bodies. In this work, major NW-SE and minor NE-SW, E-W oriented structures detected by the analytical signal are more enhanced by the tilt angle derivative method as shown in Figure 12C.

From the point of view of magnetic tilt derivative map, the areas that shows positive and zero tilt derivative signature exhibit low bearing capacity due to weak zones/fractures filled with weathered materials while those areas on the map with negative tilt angle values far from the sources are characterized by competent rocks of potentially high bearing capacity.

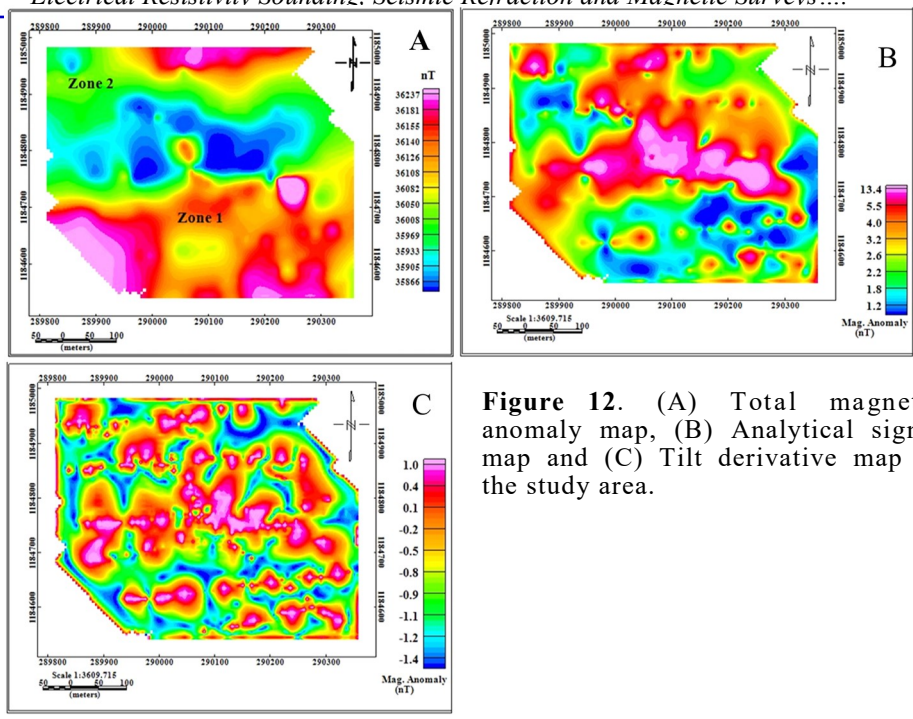

Figure 12. (A) Total magnetic anomaly map, (B) Analytical signal map and (C) Tilt derivative map of the study area.

Conclusion

Integrated geophysical survey techniques employed in this work have mapped the stratification of the subsurface from their electrical and P-wave responses. As showed through correlation with the lithological log from a neighboring borehole, the approaches have mapped the different subsurface layers. Additionally, the techniques give a 'synoptic view' of the subsurface and allow the identification of explicit areas of weakness/ discontinuity to be considered during building foundation design. The depth to the competent bedrock over the survey site and its morphology are also mapped. From the resistivity survey, it is concluded that the first four geo-electric layers have relatively low resistivity in profile-2 and profile-3 when compared to the resistivity of the corresponding layers in profile one and profile -4. This trend is observed because of the relatively high degree of weathering of rocks in the central region of the study area. As a result, rocks at the central portion of the area will have low bearing capacity. Besides, the sliced-stacked apparent resistivity section map indicates that the central and southeastern portions of the study area may deliver rocks of low bearing capacity for building foundation than the rest of the area.

The seismic refraction survey maps three subsurface layers up to a depth of 20 m. The first layer shows a P-wave velocity of 252 to 354 m/s and a thickness of 1 to 8 m. This velocity range is considered as the response of top dry soil, clayey soil, and/or highly weathered rock material. The lowest P-wave velocity values were observed at the central part of the study area. The second layer has a P-wave velocity of 906 to 1397 m/s which is the response of highly to moderately weathered and fractured basalt. The lowest P-wave velocity values of this layer are observed in the central and southeastern part of the study area. With P-wave velocity greater 1000 m/s, this layer is considered as the bedrock for foundation. The third layer has relatively high velocity (1616 to 2542 m/s) corresponding to moderately weathered and highly fractured basalt. This layer also has a relatively low velocity at the central part of the study area. Based on the P-wave velocity of the second and third layers, rocks at the central and southeastern part of the area will have low bearing capacity.

The magnetic anomaly map show a relatively high anomaly contrast between the central and other parts of the area. From this, it can be deduced that high magnetic anomaly responses are the results of relatively less weathered basaltic rocks whereas low magnetic anomaly responses are observed due to weak zones, high degree of weathering in rocks, and thick soil deposit relative to the other area. The analytical signal and the tilt derivative maps have clearly outlined localities of high magnetic gradient that results from structural discontinues (weak zones). The major structure in the study area has NW-SE orientation but minor structures have NE-SW and E-W orientation. The major structure, which is found at the central part of the site, may have an adverse effect on the stability of the building foundation. As a result, this region needs more emphasis to erect large engineering structures.

Acknowledgements

I would like to thank Dr. Fekadu Tamiru for his critical comments and technical help starting from the beginning to the completion of the study. I would like to give my heart full thanks to my friends Ynesew Asirade, Dejene Alemu, Alehegn Getnet and Mitku Mezigebu, for their encouragement and support during field data collection and data processing. I would like also to strongly acknowledge University of Gondar, Wollega University, Debre Markos University Bure town water office and West Gojam zone mineral, Energy and water office.

References

ADSWE. (2017). Groundwater source investigation for Bure Integrated Agro Industry Park water supply project: *Hydrogeology and geotechnical work process.* (Unpublished report), Bahir Dar, Ethiopia.

Bell, F.G. (2007). Engineering Geology, 2nd ed., *Butterworth*-Heinemann, Burlington.

EIGS. (2008).Geological report of Bure map sheet (NC-37/5).4

Emmanuael, T. (2015). Geotechnical site investigation using Seismic refraction and resistivity Techniques, Kwame Nkrumah University of Science and Technology.

Ibitoye F. P., Ipinmoroti F. V., Salami M., Akinluwade K. J., Taiwo A.T. and Adetunji A.R. (2013). Application of Geophysical Methods to Building Foundation Studies: *International Journal of Geosciences*, Nigeria, 2013, 4, 1256-1266.

Kearey, P., Brooks M., and Hill, L. (2002). An Introduction to Geophysical Exploration (3rd ed.). *Blackwell Science Ltd,* London, pp., 281.

Loke, M.H. (2001*).* Electrical Imaging Survey for Environmental and Engineering Studies*: A practical guide to 2D and 3D surveys.*

M. H. de Freitas (2007). Geology for Engineers (7th ed). *Imperial College of Science and Technology*, London, pp., 348.

Mohr, P.A. (1963). The geology of Ethiopia. *Haile Selassie I Univ.*, Addis Ababa, 268 p.

Olusola O., Olajumake O. and Solomon A. (2015). The use of magnetic surveying in engineering site characterization, *international journal of innovative research and development,* vol.4, issue 13, Nigeria.

Sheriff, R..E. and Geldart, L.P. (1995). Exploration Seismology (2nd ed.). *Cambridge University Press*, London, 592pp.

Sattam Almadani, Elkhedr Ibrahim, Kamal Abdelrahman, Abdulaziz Al-Bassam and Awad Al-Shmrani (2014). Magnetic and seismic refraction survey for site investigation of an urban expansion site in Abha District, Southwest Saudi Arabia, *Arab J Geosci (2015) 8:2299–2312,* Saudi Arebia.

Solomon Tadesse, Jean-Pierre Milesi and Yves Deschamps. (2003). Geology and mineral potential of Ethiopia: a note on geology and mineral map of Ethiopia, *Journal of African Earth Sciences 36 (2003) 273–313*, Addis Ababa, Ethiopia.

Tefera, M., Chernet, T. and Workeneh, H. (1996 b). Explanation to Geological Map of Ethiopia. Scale 1:2,000,000, second ed. EIGS, Addis Abbaba, 69 p.

Telford, W.M., L.P. Geldart, R.E. Sheriff and D.A. keys. (1990). Applied Geophysics, 2nd edn. *Cambridge University Press*, London, 760 pp.

Tigistu Haile and Alemayehu Ayele (2014). Electrical Resistivity Tomography and magnetic surveys: applications for building site characterization at Gubre, Wolkite University Site, and Western Ethiopia Addis Ababa University, *Ethiop. J. Sci*., 37: 13–30.